Gas-Phase Chemistry

DOI: 10.1002/ange.201302344

A Combined Experimental and Theoretical Study on the Gas-Phase Synthesis of Toluene under Single Collision Conditions**

Beni B. Dangi, Dorian S. N. Parker, Ralf I. Kaiser, Adeel Jamal, and Alexander M. Mebel*

Since its very first isolation by Pelletier and Walter in 1837,[1] the formation mechanisms and role of the toluene molecule ($C_6H_5CH_3$) **1** (Scheme 1) in extraterrestrial environments and combustion flames have received considerable attention from astrochemists[2,3] as well as from the combustion[4] and the physical-organic chemistry communities.[5–7] Toluene portrays the simplest representative of an alkyl-substituted benzene molecule with the methyl group enhancing the reactivity toward radical and electrophile aromatic substitution compared to benzene.[8] It is further considered as a crucial building block to form methyl-substituted polycyclic aromatic hydrocarbons (PAHs) such as 1- and 2-methylnaphthalene.[9–13] In combustion flames, the formation of phenylacetylene **2**, styrene **3**, and biphenyl **4** (Scheme 1) can be rationalized through phenyl addition. Atomic hydrogen is eliminated upon reaction of the phenyl radical with acetylene (C_2H_2),[14] ethylene (C_2H_4),[15] and benzene (C_6H_6).[16] The analogous reaction of the phenyl radical with methane (CH_4) does not lead to toluene, but solely to benzene plus a methyl radical (CH_3) through hydrogen abstraction.[17] Consequently, the formation routes of toluene in combustion flames and in the interstellar medium have not been unraveled to date. Here, we show that the reaction of the ethynyl radical (CCH; C_2H) with isoprene (2-methyl-1,3-butadiene; C_5H_8) presents a facile, barrierless route to the toluene molecule in a single collision event in the gas phase through the reaction of two acyclic precursor molecules. This reaction is also of interest to the physical-organic chemistry community since it represents a benchmark system to untangle the formation of a methyl-substituted aromatic molecule through radical substitution reactions involving successive isomerizations through cyclization and hydrogen shifts.

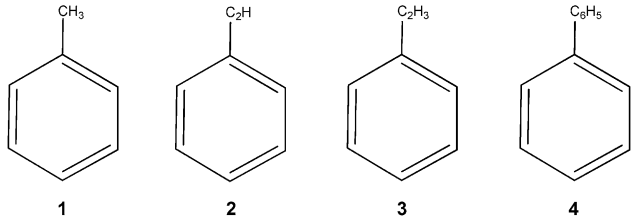

Scheme 1. Toluene **1**, phenylacetylene **2**, styrene **3**, and biphenyl **4**.

Reactive scattering signal from the reaction of [D_1]ethynyl radical $C_2D(X^2\Sigma^+)$ with isoprene (C_5H_8; X^1A') was monitored at mass-to-charge ratios (m/z) of 93 ($C_7H_7D^+$), 92 ($C_7H_6D^+/C_7H_8^+$), and 91 ($C_7H_5D^+/C_7H_7^+$). The signal at $m/z = 93$ originates from the C_7H_7D product(s) formed through atomic hydrogen loss, whereas ion counts at $m/z = 92$ could have two contributions: an atomic deuterium loss connected to the formation of C_7H_8 products or dissociative ionization of C_7H_7D products in the electron impact ionizer of the detector. The signal at $m/z = 91$ may depict two contributions from dissociative electron impact ionization of C_7H_7D and/or C_7H_6D product molecules. However, all data could be fit with the product mass combinations of 93 amu (C_7H_7D) plus 1 amu (H). This finding suggests the existence of a [D_1]ethynyl (C_2D, 26 amu) versus atomic hydrogen replacement channel and the gas-phase synthesis of a molecule with the molecular formula C_7H_7D (Figure 1). Considering that the [D_1]ethynyl reactant does not have a hydrogen atom, the hydrogen atom is emitted from the isoprene molecule. The laboratory angular distribution (Figure 2) extends at least 40° within the scattering plane and peaks close to the center-of-mass angle at 41.1 ± 1.2°. These results suggest indirect scattering dynamics through C_7H_8D complex(es).

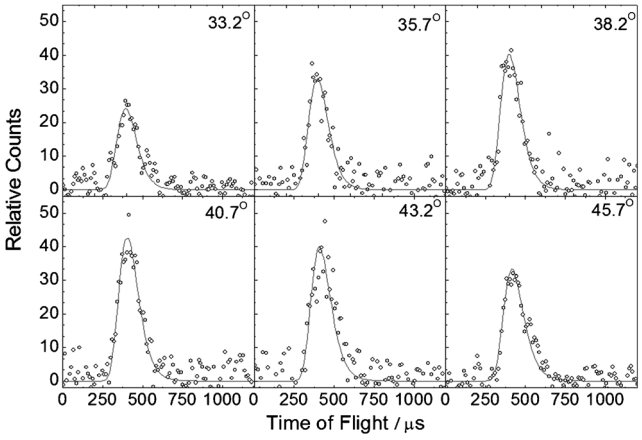

Figure 1. Time-of-flight spectra of reactively scattered species recorded at mass-to-charge, m/z, 93 ($C_7H_7D^+$) in the reaction of [D_1]ethynyl radicals with isoprene. The circles represent the experimental data, and the solid line represents the best fit to the data.

[*] Dr. B. B. Dangi, Dr. D. S. N. Parker, Prof. R. I. Kaiser
Department of Chemistry, University of Hawai'i at Manoa
Honolulu, HI 96822 (USA)
E-mail: ralfk@hawaii.edu
Homepage: http://www.chem.hawaii.edu/Bil301/welcome.html
Dr. A. Jamal, Prof. A. M. Mebel
Department of Chemistry and Biochemistry
Florida International University
Miami, FL 33199 (USA)

[**] This work was supported by the US Department of Energy, Basic Energy Sciences, via grants DE-FG02-03ER15411 (Hawaii) and DE-FG02-04ER15570 (Florida).

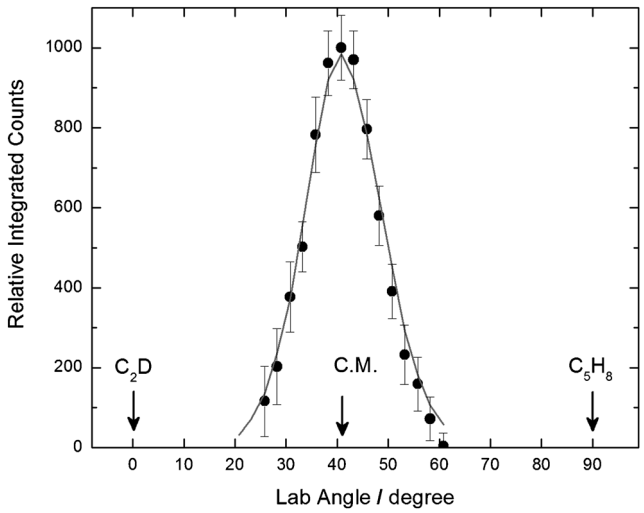

Figure 2. Laboratory frame angular distribution of reactively scattered species recorded at mass-to-charge, m/z, 93 ($C_7H_7D^+$) in the reaction of [D_1]ethynyl radicals with isoprene. C.M. designates the center-of-mass angle. Full circles represent the experimental data while the solid line represents the calculated distribution.

Having established that the reaction of the [D_1]ethynyl radical with isoprene leads to C_7H_7D(s) plus atomic hydrogen, we extract now information on the reaction mechanism. The center-of-mass (CM) translational energy distribution, $P(E_T)$, and the angular distribution, $T(\theta)$, (Figure 3) help us to gain these insights. The maximum translational energy, $E_{max,}$ of 420 ± 45 kJ mol^{-1} reflects the sum of the reaction energy plus the collision energy for those molecules born without internal

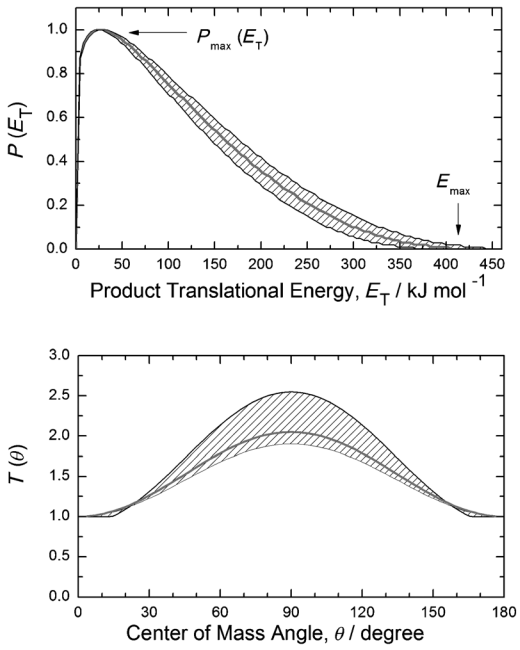

Figure 3. Center-of-mass translational-energy-flux distribution (upper) and angular-flux distribution (lower) for the hydrogen atom loss channel in the reaction of [D_1]ethynyl with isoprene leading to C_7H_7D isomer(s). The hatched areas indicate the acceptable upper and lower limits of the fits accounting for the error limits and the gray solid line defines the best-fit function.

excitation. After the subtraction of the collision energy of 51.3 ± 1.8 kJ mol^{-1}, the reaction is determined to be exoergic by 369 ± 47 kJ mol^{-1}. Further, the translational energy distribution shows a distribution maximum ($P_{max}(E_T)$) around 25 kJ mol^{-1} indicating a tight exit transition state of the decomposing collision complex. Finally, 30 ± 5 % of the available energy is released, on average, into the translational degrees of freedom of the reaction products. This order of magnitude indicates indirect scattering dynamics. We are gaining additional information on the reaction dynamics from the center-of-mass angular distribution. This distribution depicts intensity over the complete angular range from 0° to 180° suggesting indirect scattering dynamics through C_7H_8D reaction intermediate(s).[18] Further, the $T(\theta)$ distribution is forward–backward symmetric with respect to 90° indicating a long-lived intermediate(s). Finally, the distribution maximum at 90° hints to geometrical constraints in the reaction so that the hydrogen atom is ejected almost perpendicular to the rotational plane of the decomposing complex.[19]

In case of polyatomic reactants, it is useful to merge the results from the crossed-beam experiments with electronic structure calculations (Figure 4). The calculations were conducted for the reaction of ethynyl with isoprene; the replacement of the hydrogen atom by a deuterium in ethynyl results in energetics, which differ because of distinct zero-point vibrational energies, by less than 2 kJ mol^{-1}. The ethynyl radical adds without any entrance barrier to any of the four chemically nonequivalent carbon atoms C1 to C4 of the isoprene reactant leading to intermediates INT1 to INT4. These intermediates undergo unimolecular decomposition through atomic hydrogen and/or methyl group loss yielding six noncyclic reaction products (p1–p6) in overall exoergic (40–150 kJ mol^{-1}) reactions. The electronic structure calculations also identified reaction pathways to two cyclic reaction products: benzene (C_6H_6) and toluene ($C_6H_5CH_3$) formed by a methyl group and atomic hydrogen losses (Figure 4b). Both intermediates INT1 and INT4 can isomerize through ring closures leading to INT5 and INT6. These isomers are interconnected by a [3,4]-hydrogen shift. Considering the energetics and barrier heights, the addition of the ethynyl radical to either C1 or to C4 leads eventually to INT5 and INT6. The latter were found to undergo facile hydrogen shifts to INT7 and INT8. These intermediates decompose by atomic hydrogen loss forming toluene in an overall exoergic reaction (370 kJ mol^{-1}). An alternative reaction pathway from INT8 involves a hydrogen shift to INT9. However, the competing transition state in the decomposition of INT8 to toluene plus atomic hydrogen lies 90 kJ mol^{-1} below the transition state connecting INT8 and INT9. Therefore, we can predict that INT8 should fragment to the products rather than isomerize to INT9. Since INT9 is suggested to be not accessible, so are the pathways from INT9 to toluene plus atomic hydrogen and benzene plus the methyl radical.

We are merging now the experimental and theoretical data to gain an understanding of the underlying reaction dynamics and of the reaction mechanism(s). A comparison of the experimentally determined reaction energy of 369 ± 47 kJ mol^{-1} with the reaction energies to form isomers p1 to p7 suggests that [D_1]toluene plus atomic hydrogen (p7′ + p7″)

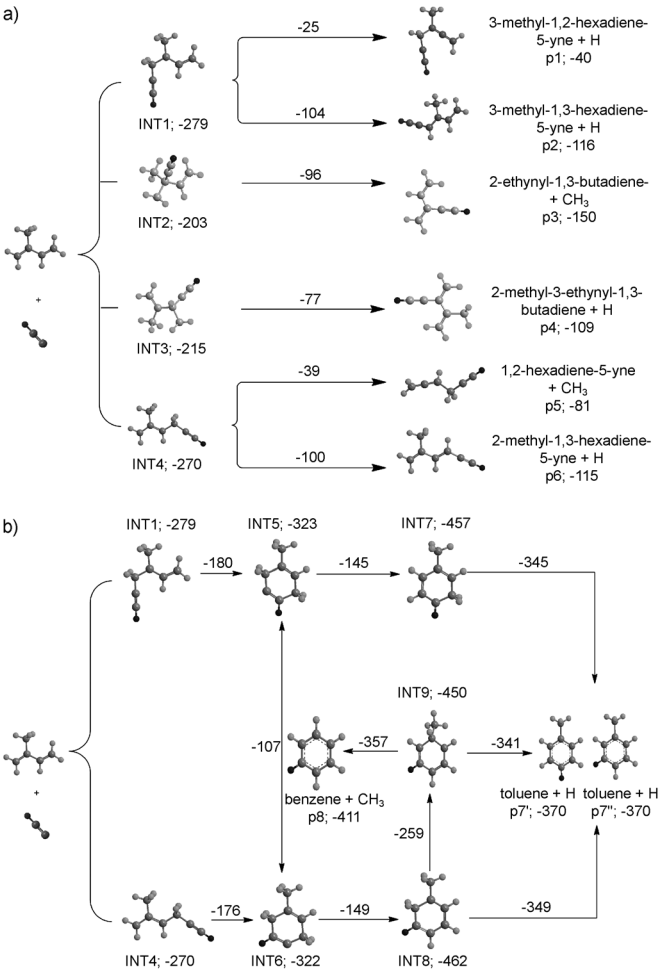

Figure 4. Lowest energy pathways on the doublet C_7H_8D potential energy surface (PES) leading to a) noncyclic and b) cyclic reaction products. All energies are given in kJ mol^{-1} relative to the reactant energies. Deuterium atoms have been colored in black.

are synthesized. The computed energetics of 370 ± 5 kJ mol^{-1} correlate well with the experimental data of 369 ± 47 kJ mol^{-1}; the thermodynamically less stable isomers are associated with reaction exoergicities of -40 to -116 kJ mol^{-1} and cannot account for the experimental data alone. However, we cannot discount that besides [D_1]toluene, p1, p2, p4, and/or p6 are also synthesized. The reaction of the [D_1]ethynyl radical with isoprene follows indirect scattering dynamics and is initiated by a barrierless addition of the [D_1]ethynyl radical to the sterically more accessible C1 and/or C4 carbon atoms of the isoprene molecule leading to INT1 and INT4, which isomerize by ring closure to INT5 and INT6, respectively. Successive hydrogen shifts yield INT7 and INT8, which decompose through atomic hydrogen losses from the C4 and C1 carbon atoms yielding two toluene isotopologues (p7′, p7″). For both pathways, tight exit transition states located 25 and 21 kJ mol^{-1} above the separated products were predicted; considering the distribution maximum of the center-of-mass translational energy distribution of 25 kJ mol^{-1}, our experiments fully support the existence of tight exit transition state(s). Further, the center-of-mass angular distribution indicates that the hydrogen atom is emitted almost perpendicularly to the decomposing intermediates; these results are verified by our computations depicting angles of about 82° of the atomic hydrogen loss from INT7 and INT8 (Figure 5). Finally, our statistical

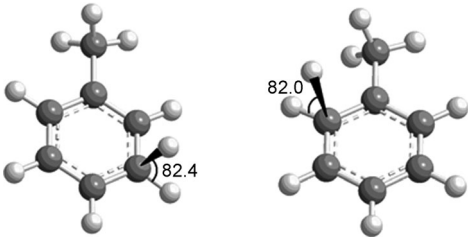

Figure 5. Computed geometries of the exit transition state leading to the formation of [D_1]toluene from intermediates INT7 and INT8.

calculations support the formation of toluene as well. Considering an initial population of INT1 and INT4, fractions of 34 and 52% toluene formation are expected, with toluene being formed predominantly through INT5 and INT6 under our experimental conditions. These calculations further suggest that in case of INT1 and INT4, 66 and 48% of the acyclic reaction products p2 and p6 are formed.

In summary, we have elucidated the chemical dynamics of the formation of [D_1]toluene through a single collision event of two neutral, noncyclic precursor molecules in the gas phase. Since the reaction has no entrance barrier, is exoergic, and all transition states involved are located below the energy of the separated reactants, the reaction of ethynyl radicals with isoprene can also lead to toluene not only in high-temperature combustion flames, but also in low-temperature environments such as in the cold molecular cloud TMC-1. The substitution of the methyl group at the C2 carbon atom of isoprene by any alkyl group might lead to the synthesis of alkyl-substituted benzene molecules. This reaction class presents therefore a facile and compelling alternative to the formation of alkyl benzenes through reactions of benzene with alkyl radicals with the latter being initiated only after passing an entrance barrier to reaction. Consequently, a hitherto unknown pathway to the formation of toluene and alkyl-substituted benzenes is presented underscoring the importance of ethynyl-radical-mediated formation of aromatic molecules in combustion flames from acyclic precursors through barrierless and strongly exoergic reactions from noncyclic precursor molecules.

Materials and Methods

Experimental section: The experiments were conducted under single collision conditions using a crossed molecular beam apparatus.[20] [D_1]ethynyl radicals were generated through laser ablation of graphite and seeding the ablated species in molecular deuterium. The latter acted as a seeding and reactant gas. The molecular beam passed a skimmer and a four-slot chopper wheel, which selected a segment of the pulsed C_2D ($X^2\Sigma^+$) beam of a well-defined peak velocity ($v_p = 2240 \pm 40$ ms^{-1}) and speed ratio ($S = 2.9 \pm 0.5$). The [D_1]ethynyl beam crossed a pulsed isoprene (C_5H_8; X^1A') beam ($v_p = 740 \pm 10$ ms^{-1}, $S =$

8.5 ± 0.2) perpendicularly in the interaction region at a collision energy of 51.3 ± 1.8 kJ mol^{-1}. The reaction products were analyzed by a rotatable mass spectrometer operated in the time-of-flight mode and ionized by electron impact at 80 eV, passed a quadrupole mass filter, and reached a Daly-type ion detector. The time-of-flight (TOF) spectra were recorded at multiple angles and then integrated to obtain the laboratory angular distribution. A forward-convolution routine was used to fit the experimental data.[20]

Electronic structure calculations: The reactants, intermediates, transition states, and products on the C_7H_8D potential energy surface (PES) of the reaction of C_2D with isoprene were calculated using the hybrid density functional B3LYP[21] with the 6-311G(d,p) basis set. Optimized Cartesian coordinates, unscaled vibrational frequencies, moments of inertia, and zero-point energies (ZPE) were obtained at this level of theory. The optimized Cartesian coordinates of all species were used as single-point coupled cluster CCSD(T) calculations[22] with Dunning's correlation-consistent cc-pVTZ basis set.[23] The GAUSSIAN 09[24] and MOLPRO 2010[25] program packages were employed to carry out B3LYP and CCSD(T) calculations.

Received: March 20, 2013
Published online: June 3, 2013

Keywords: ab initio calculations · combustion chemistry · gas-phase chemistry · radicals · reaction dynamics

[1] P.-J. Pelletier, P. Walter, *Ann. Chim. Phys.* **1837**, *67*, 269.
[2] J. J. Newby, J. A. Stearns, C. P. Liu, T. S. Zwier, *J. Phys. Chem. A* **2007**, *111*, 10914.
[3] G. E. Douberly, A. M. Ricks, P. V. R. Schleyer, M. A. Duncan, *J. Phys. Chem. A* **2008**, *112*, 4869.
[4] M. Kamphus, M. Braun-Unkhoff, K. Kohse-Hoinghaus, *Combust. Flame* **2008**, *152*, 28.
[5] E. Borrás, L. A. Tortajada-Genaro, *Atmos. Environ.* **2012**, *47*, 154.
[6] C. Han, Y. Liu, C. Liu, J. Ma, H. He, *J. Phys. Chem. A* **2012**, *116*, 4129.
[7] C. A. Stroud, P. A. Makar, D. V. Michelangeli, M. Mozurkewich, D. R. Hastie, J. Humble, *Environ. Sci. Technol.* **2004**, *38*, 1471.
[8] B. Galabov, G. Koleva, H. F. Schaefer, P. V. Schleyer, *J. Org. Chem.* **2010**, *75*, 2813.
[9] S. Thomas, M. J. Wornat, *Fuel* **2008**, *87*, 768.
[10] P. Schmitt-Kopplin, Z. Gabelica, R. D. Gougeon, A. Fekete, B. Kanawati, M. Harir, I. Gebefuegi, G. Eckel, N. Hertkorn, *Proc. Natl. Acad. Sci. USA* **2010**, *107*, 2763.
[11] F. Salama, G. A. Galazutdinov, J. Krelowski, L. J. Allamandola, F. A. Musaev, *Astrophys. J.* **1999**, *526*, 265.
[12] A. M. Ricks, G. E. Douberly, M. A. Duncan, *Astrophys. J.* **2009**, *702*, 301.
[13] B. J. Finlayson-Pitts, J. N. Pitts, Jr., *Science* **1997**, *276*, 1045.
[14] X. B. Gu, F. T. Zhang, Y. Guo, R. I. Kaiser, *Angew. Chem.* **2007**, *119*, 6990; *Angew. Chem. Int. Ed.* **2007**, *46*, 6866.
[15] F. Zhang, X. Gu, Y. Guo, R. I. Kaiser, *J. Org. Chem.* **2007**, *72*, 7597.
[16] F. T. Zhang, X. B. Gu, R. I. Kaiser, *J. Chem. Phys.* **2008**, *128*.
[17] I. V. Tokmakov, J. Park, S. Gheyas, M. C. Lin, *J. Phys. Chem. A* **1999**, *103*, 3636.
[18] R. I. Kaiser, C. Ochsenfeld, M. Head-Gordon, Y. T. Lee, A. G. Suits, *Science* **1996**, *274*, 1508.
[19] W. B. Miller, S. A. Safron, D. R. Herschbach, *Disscuss. Faraday Soc.* **1967**, *44*, 108.
[20] X. Gu, Y. Guo, F. Zhang, A. M. Mebel, R. I. Kaiser, *Faraday Discuss.* **2006**, *133*, 245.
[21] A. D. Becke, *J. Chem. Phys.* **1993**, *98*, 5648.
[22] G. D. Purvis, R. J. Bartlett, *J. Chem. Phys.* **1982**, *76*, 1910.
[23] T. H. Dunning, *J. Chem. Phys.* **1989**, *90*, 1007.
[24] M. J. Frisch, G. W. Trucks, H. B. Schlegel, G. E. Scuseria, M. A. Robb, J. R. Cheeseman, G. Scalmani, V. Barone, B. Mennucci, G. A. Petersson, H. Nakatsuji, M. Caricato, X. Li, H. P. Hratchian, A. F. Izmaylov, J. Bloino, G. Zheng, J. L. Sonnenberg, M. Hada, M. Ehara, K. Toyota, R. Fukuda, J. Hasegawa, M. Ishida, T. Nakajima, Y. Honda, O. Kitao, H. Nakai, T. Vreven, J. A. Montgomery, Jr., J. E. Peralta, F. Ogliaro, M. Bearpark, J. J. Heyd, E. Brothers, K. N. Kudin, V. N. Staroverov, R. Kobayashi, J. Normand, K. Raghavachari, A. Rendell, J. C. Burant, S. S. Iyengar, J. Tomasi, M. Cossi, N. Rega, J. M. Millam, M. Klene, J. E. Knox, J. B. Cross, V. Bakken, C. Adamo, J. Jaramillo, R. Gomperts, R. E. Stratmann, O. Yazyev, A. J. Austin, R. Cammi, C. Pomelli, J. W. Ochterski, R. L. Martin, K. Morokuma, V. G. Zakrzewski, G. A. Voth, P. Salvador, J. J. Dannenberg, S. Dapprich, A. D. Daniels, Ö. Farkas, J. B. Foresman, J. V. Ortiz, J. Cioslowski, and D. J. Fox, Gaussian, Inc, Wallingford CT, **2009**.
[25] H.-J. Werner, P. J. Knowles, G. Knizia, F. R. Manby, M. Schütz, P. Celani, T. Korona, R. Lindh, A. Mitrushenkov, G. Rauhut, K. R. Shamasundar, T. B. Adler, R. D. Amos, A. Bernhardsson, A. Berning, D. L. Cooper, M. J. O. Deegan, A. J. Dobbyn, F. Eckert, E. Goll, C. Hampel, A. Hesselmann, G. Hetzer, T. Hrenar, G. Jansen, C. Köppl, Y. Liu, A. W. Lloyd, R. A. Mata, A. J. May, S. J. McNichols, W. Meyer, M. E. Mura, A. Nicklaß, D. P. O'Neill, P. Palmieri, D. Peng, K. Pflüger, R. Pitzer, M. Reiher, T. Shiozaki, H. Stoll, A. J. Stone, R. Tarroni, T. Thorsteinsson, M. Wang 2010 ed., **2010**, http://molpro.net.

